

Article

Effect of Molecular Structure of Organic Acids on the Crystal Habit of α -CaSO₄·0.5H₂O from Phosphogypsum

Xianbo Li ^{1,2,3} and Qin Zhang ^{1,2,3,*}¹ Mining College, Guizhou University, Guiyang 550025, China; xbli1990@163.com² National & Local Joint Laboratory of Engineering for Effective Utilization of Regional Mineral Resources from Karst Areas, Guiyang 550025, China³ Guizhou Key Lab of Comprehensive Utilization of Nonmetallic Mineral Resources, Guiyang 550025, China

* Correspondence: qzhang@gzu.edu.cn

Received: 22 November 2019; Accepted: 4 January 2020; Published: 6 January 2020



Abstract: The organic acid crystal modifiers play an important role in the control of the crystal habit of α -hemihydrate gypsum (α -CaSO₄·0.5H₂O) from phosphogypsum, but the molecular structure characteristics of crystal modifiers have not been clarified, which makes it difficult to judge whether an organic acid has the ability to regulate the crystal habit of α -CaSO₄·0.5H₂O directly. In this work, the effect of organic acids with different molecular structures on the crystal habit of α -CaSO₄·0.5H₂O and its adsorption differences onto the α -CaSO₄·0.5H₂O surface were explored. The results show that the molecular structure characteristics of crystal modifiers contain two or more carboxylic groups (COOH) that are separated by two methylene or methine groups. Furthermore, organic acids with the regulation ability can adsorb on the surface of α -CaSO₄·0.5H₂O and change its growth habit. With the increase in the crystal modifier concentration, the α -CaSO₄·0.5H₂O crystals are shortened in length and enlarged in width, resulting in the decrease in aspect ratio and the increase in compressive strength. Conversely, when the adsorption of ineffective organic acids on the surface of α -CaSO₄·0.5H₂O was not detected, the α -CaSO₄·0.5H₂O crystals remained long hexagonal prisms. These results have guiding significance for the screening of novel organic acid crystal modifiers.

Keywords: α -hemihydrate gypsum; crystal habit; organic acid; crystal modifier; molecular structure; phosphogypsum

1. Introduction

Phosphogypsum (PG) is an industrial solid waste produced during the production of phosphoric acid from phosphate ore [1,2], which is an important renewable gypsum resource. The main constituent of PG is calcium sulfate dihydrate (CaSO₄·2H₂O), but it also contains impurities such as soluble phosphate, co-crystallized phosphorus, soluble fluoride, and organic matters as well as heavy metals and radionuclides [3–6]. The utilization of PG is severely restricted by these harmful impurities, so the comprehensive utilization rate is only 39.7% [7]. Currently, the preparation of α -hemihydrate gypsum (α -CaSO₄·0.5H₂O) using PG as the raw material is an important direction for its high value-added utilization. α -CaSO₄·0.5H₂O has excellent mechanical strength, work performance, and environmental performance, which has been widely used in precision casting, high-end ceramics, functional filler, decorative materials, and so on [8,9]. However, the impurities have a detrimental effect on the preparation of α -CaSO₄·0.5H₂O; the soluble phosphate and co-crystallized phosphorus can decrease the slurry pH and retard the hydration of α -CaSO₄·0.5H₂O, and then reduce the strength of hardened gypsum. Similarly, the soluble fluoride can decrease the gypsum strength [10]. Therefore, PG should be pretreated to remove the soluble impurities. In addition, the radionuclides of PG are derived from

phosphate ores, mainly Ra^{226} , Th^{232} , and K^{40} , and the radioactivity of PG must meet the standard of GB 6566-2010 (limits of radionuclides in building materials) in order for it to be used as a building material. Notably, the crystal habit is one of the most important factors for affecting the mechanical strength of $\alpha\text{-CaSO}_4\cdot 0.5\text{H}_2\text{O}$ [11–14]. Compared with the needle-shaped $\alpha\text{-CaSO}_4\cdot 0.5\text{H}_2\text{O}$, the short columnar $\alpha\text{-CaSO}_4\cdot 0.5\text{H}_2\text{O}$ with a low aspect ratio and a large width shows better mechanical strength [15]. Therefore, the key to the preparation of $\alpha\text{-CaSO}_4\cdot 0.5\text{H}_2\text{O}$ is to select a suitable crystal modifier to control the crystal habit of $\alpha\text{-CaSO}_4\cdot 0.5\text{H}_2\text{O}$.

Many studies have proven that some organic acids can be used as a crystal modifier to regulate the crystal shape of $\alpha\text{-CaSO}_4\cdot 0.5\text{H}_2\text{O}$ particles. For instance, the short hexagonal prism $\alpha\text{-CaSO}_4\cdot 0.5\text{H}_2\text{O}$, with an aspect ratio of 1.0–1.4, could be obtained by adding succinic acid ($\text{C}_4\text{H}_6\text{O}_4$) [15–18] and sodium succinate ($\text{C}_4\text{H}_4\text{O}_4\text{Na}_2\cdot 6\text{H}_2\text{O}$) [19]. The pilot scale tests further demonstrated that $\alpha\text{-CaSO}_4\cdot 0.5\text{H}_2\text{O}$ with an aspect ratio of 2.8–3.2 can be synthesized by adding a small amount of $\text{C}_4\text{H}_6\text{O}_4$ and sodium borate ($\text{Na}_2\text{B}_4\text{O}_7\cdot 5\text{H}_2\text{O}$) [20]. In the presence of maleic acid ($\text{C}_4\text{H}_4\text{O}_4$), the crystal habit of $\alpha\text{-CaSO}_4\cdot 0.5\text{H}_2\text{O}$ evolved from a needle-like whisker to a short equiaxial crystal [21]. The crystal habit of $\alpha\text{-CaSO}_4\cdot 0.5\text{H}_2\text{O}$ crystals can be influenced by adding citric acid ($\text{C}_6\text{H}_8\text{O}_7\cdot \text{H}_2\text{O}$) [22] and sodium citrate ($\text{Na}_3\text{C}_6\text{H}_5\text{O}_7\cdot 2\text{H}_2\text{O}$) [12,13]; the aspect ratio of $\alpha\text{-CaSO}_4\cdot 0.5\text{H}_2\text{O}$ crystal is decreased from 10.3 to 0.6 with the increase in the sodium citrate dosage from 0 to 0.045 wt% [23]. Recently, Li et al. [24] found that L-aspartic acid ($\text{C}_4\text{H}_7\text{NO}_4$) is an effective crystal modifier for regulating the crystal shape of $\alpha\text{-CaSO}_4\cdot 0.5\text{H}_2\text{O}$. Additionally, Wang et al. [25] demonstrated that disodium ethylenediamine tetraacetate ($\text{C}_{10}\text{H}_{14}\text{N}_2\text{Na}_2\text{O}_8$) influences the crystal habit and nucleation of $\alpha\text{-CaSO}_4\cdot 0.5\text{H}_2\text{O}$. In particular, Badens et al. [26] investigated the influence of different organic additives on the morphology of gypsum crystals where the results showed that there is an obvious relationship between the rate retarding effect and structural matching between the crystal faces involved and the conformation of the molecule of the additive. The acicular gypsum crystals in pure solution transformed into flat crystals with much more twinned crystals in the presence of malic acid at 1000 ppm.

Nevertheless, not all organic acids possess the ability to control the crystal shape of $\alpha\text{-CaSO}_4\cdot 0.5\text{H}_2\text{O}$, and only a few reports have been published regarding the molecular structure characteristics of organic acids as crystal modifiers. This makes it difficult to determine, without testing, whether an organic acid has the ability to regulate the crystal habit of $\alpha\text{-CaSO}_4\cdot 0.5\text{H}_2\text{O}$, and a considerable amount of experimental work is needed to confirm the effectiveness of organic acids. Therefore, the effects of organic acids with different molecular structures on the crystal habit and mechanical properties of $\alpha\text{-CaSO}_4\cdot 0.5\text{H}_2\text{O}$ were systematically investigated. The organic acids used in this paper can be divided into three families: benzenedicarboxylic acids, amino acids, and straight-chain dicarboxylic acids. According to the comparative research of benzenedicarboxylic acids and straight-chain dicarboxylic acids, the effect of different carbon chain lengths between two carboxylic groups (COOH) on the crystal habit of $\alpha\text{-CaSO}_4\cdot 0.5\text{H}_2\text{O}$ can be clarified. Based on the amino acids, the effect of the number of COOH and the feasibility of the amino group (NH_2) instead of a hydroxyl group (OH) linked to the carbonyl group ($\text{C}=\text{O}$) on the crystal morphology can be clearly defined. Furthermore, the adsorption differences of organic acids on the surface of $\alpha\text{-CaSO}_4\cdot 0.5\text{H}_2\text{O}$ particles were also discussed. The findings have a certain guiding significance for the screening or design and synthesis of novel organic acid crystal modifiers purposefully.

2. Materials and Methods

2.1. Materials

Analytical grade calcium chloride (CaCl_2) and organic acids were obtained from Sinopharm Chemical Reagent Co. Ltd., Shanghai, China. PG was collected from the Wengfu (Group) Co. Ltd., Guizhou Province, China. The x-ray diffraction analysis indicated that the main phase of PG is $\text{CaSO}_4\cdot 2\text{H}_2\text{O}$ with a little quartz (SiO_2) and co-crystallized phosphorus ($\text{CaHPO}_4\cdot 2\text{H}_2\text{O}$). The contents of the $\text{CaSO}_4\cdot 2\text{H}_2\text{O}$, soluble phosphate and soluble fluorine were 91.32 wt%, 0.18 wt%, and 0.01 wt%,

respectively [21]. In order to reduce the influence of soluble impurities on the preparation process and mechanical strength of α -CaSO₄·0.5H₂O, the soluble phosphate and soluble fluoride were solidified by adding 0.6 wt% quicklime (mass ratio of lime to PG), and the removal rates were 90.45% and 36.36%, respectively.

Radionuclides exceeding the standard of GB 6566-2010 are one of the important factors restricting the utilization of solid waste resources. PG generally contains a small amount of radionuclides, and the radioactivity level of PG varies from region to region. Therefore, the specific activity of PG should be tested before it is used. The results are shown in Table 1 where it can be seen that the radioactivity of PG meets the requirements of the main materials for building and class A decorative materials (GB 6566-2010). Therefore, PG can be used to prepare α -CaSO₄·0.5H₂O cementitious materials.

Table 1. Radioactivity of phosphogypsum (PG).

Items	Radioactivity Nuclide Specific Activity			Internal Exposure Index	External Exposure Index
	²²⁶ Ra	²³² Th	⁴⁰ K		
PG	61.0	2.3	3.3	0.31	0.17
Main materials for building				≤1.0	≤1.0
Class A decorative materials				≤1.0	≤1.3

2.2. Preparation of α -CaSO₄·0.5H₂O Crystals

The atmospheric salt solution method was adopted to prepare α -CaSO₄·0.5H₂O powders. The hydrothermal reaction was carried out in the CaCl₂ solution, and the original solution pH was 8.6. First, 1.5 L of 2.97 M CaCl₂ and different concentrations of organic acid mixed solutions were preheated by oil bath in a 2.0 L three-mouth flask. The solution temperature was monitored by a thermometer inserted into the reactor and maintained with a deviation of ±0.5 °C. Then, 500 g of pretreatment PG was added into the mixed solutions when the temperature reached 95 °C, and the slurry in the reactor was stirred at a rate of 200 r/min. During the experiments, 10 mL of the suspension was sampled at 30 min intervals to observe the crystal habit of the reaction product.

2.3. Characterization Methods

The crystal habit of the α -CaSO₄·0.5H₂O particles was observed by a scanning electronic microscope (SEM, SU8010, Hitachi, Japan). The length and width of the α -CaSO₄·0.5H₂O particles were measured by the image analysis software Image-Pro Plus, and at least 100 particles were counted to calculate the average aspect ratio of α -CaSO₄·0.5H₂O particles. The length, width, and aspect ratio data are shown as the “mean value ± standard deviation of the mean”.

Fourier transform infrared spectroscopy (FTIR, VERTEX 70, Bruker, Germany) was adopted to clarify the adsorption of organic acids on the surface of α -CaSO₄·0.5H₂O particles. The α -CaSO₄·0.5H₂O powders prepared with different organic acids were further ground to ~5 μm and then mixed with KBr. The spectra were recorded with a scanning range from 400 to 4000 cm⁻¹ at room temperature. The adsorption of the organic acids on the surface of the α -CaSO₄·0.5H₂O particles was analyzed by the change in the characteristic adsorption peaks in the spectra.

The as-prepared α -CaSO₄·0.5H₂O powders were mixed with deionized water to form a slurry. Then, the slurry was poured into iron molds, which were vibrated ten times to remove bubbles in the slurry. After being maintained for 2 h, the iron molds were removed, and the plasters were cured for 24 h at 20 ± 2 °C and 65 ± 5% RH. Finally, the plasters were dried to a constant weight in an oven with the temperature set to 40 ± 1 °C, and the compressive strength of the hardened pastes were determined by a microcomputer-controlled compressive testing machine (YAW-300B, Zhejiang Yingsong Instrument and Equipment Manufacturing Co. Ltd., China).

3. Results and Discussion

3.1. Effect of Benzenedicarboxylic Acid on the Crystal Habit of α -CaSO₄·0.5H₂O

The benzenedicarboxylic acid (BA, HOOC₆H₄COOH) has three kinds of isomers: phthalic acid (PA), isophthalic acid (IPA), and terephthalic acid (TA), the molecular structural formulas of which are shown in Figure 1. The PA, IPA, and TA molecules contain two COOH, but the separation between the two COOH are different. At this time, using BA as a crystal modifier for the preparation of α -CaSO₄·0.5H₂O has not been reported yet, based on the available literature.

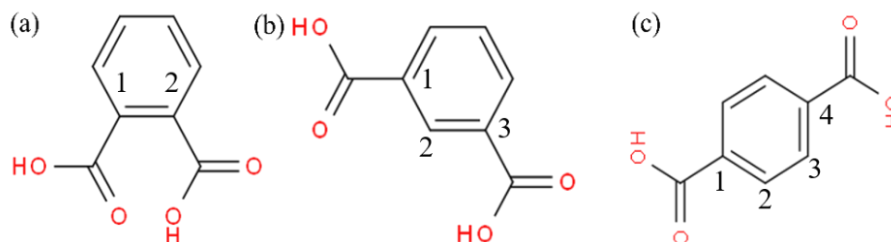


Figure 1. Molecular structural formula of (a) PA, (b) IPA, and (c) TA.

The effects of BA on the crystal habit and size of α -CaSO₄·0.5H₂O crystals are presented in Figure 2 and Table 2, respectively. The crystal habit of α -CaSO₄·0.5H₂O crystals were significantly affected by PA concentration. In the absence of PA, α -CaSO₄·0.5H₂O exists as a long columnar crystal, the average length and width of which were $59.04 \pm 14.08 \mu\text{m}$ and $11.04 \pm 3.64 \mu\text{m}$, respectively, while the aspect ratio reached 5.74 ± 1.84 . In addition, the XRD pattern of the reaction product matched well with the standard pattern of α -CaSO₄·0.5H₂O (Joint Committee on Powder Diffraction Standards (JCPDS) card 41-0224), and no characteristic peaks of CaSO₄·2H₂O (JCPDS card 33-0311) were present (Figure 3). The results indicate that the PG was completely transformed into α -CaSO₄·0.5H₂O.

The α -CaSO₄·0.5H₂O crystals were shortened in length and enlarged in width with an increase in PA concentration. In the presence of 0.07 mM PA, the average length of the α -CaSO₄·0.5H₂O particles shortened to $42.56 \pm 10.02 \mu\text{m}$, the width increased to $16.09 \pm 3.55 \mu\text{m}$, and the aspect ratio was decreased to 2.72 ± 0.70 . With a further increase in PA concentration to 0.20 mM, the average length and width of the α -CaSO₄·0.5H₂O particles were $32.19 \pm 6.87 \mu\text{m}$ and $20.73 \pm 5.26 \mu\text{m}$, respectively, and the corresponding aspect ratio decreased to 1.61 ± 0.39 . Accordingly, it can be concluded that PA is an effective crystal modifier to control the crystal habit of α -CaSO₄·0.5H₂O. However, it is interesting to note that the growth habits of α -CaSO₄·0.5H₂O were nearly unchanged at 0.20 mM IPA and TA; α -CaSO₄·0.5H₂O remained a long columnar crystal, the average width was close to 10 μm , and the aspect ratios were 4.24 ± 1.43 and 4.54 ± 1.60 , respectively. Consequently, the crystal shape of α -CaSO₄·0.5H₂O particles cannot be regulated by IPA and TA.

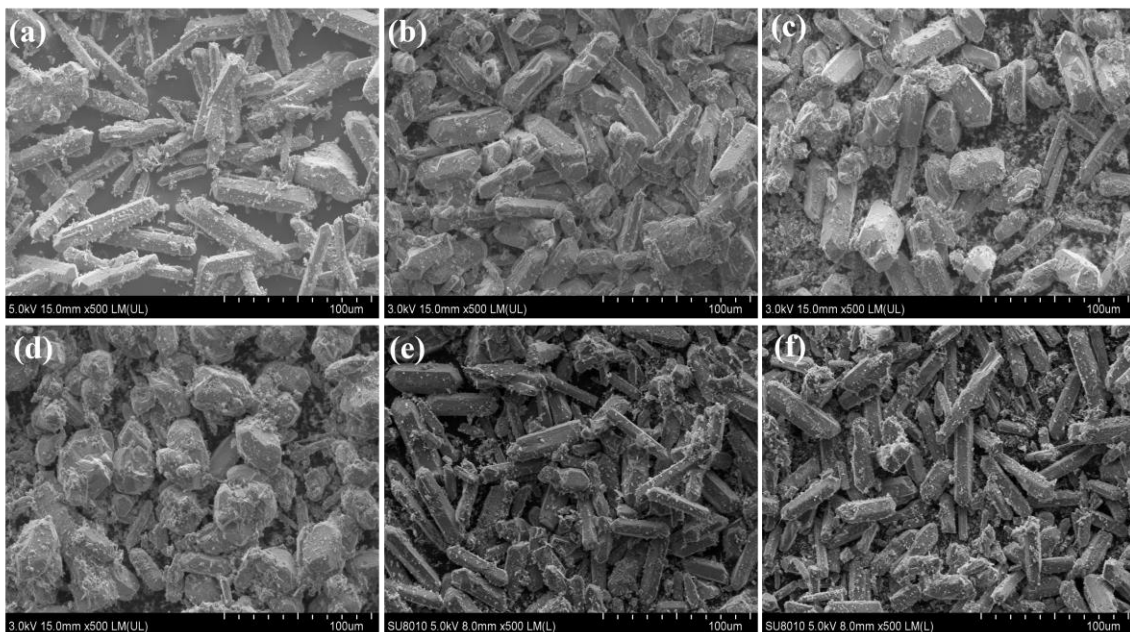


Figure 2. Effect of BA on the crystal habit of $\text{CaSO}_4 \cdot 0.5\text{H}_2\text{O}$. (a) 0 mM; (b) PA: 0.07 mM; (c) PA: 0.13 mM; (d) PA: 0.20 mM; (e) IPA: 0.20 mM; (f) TA: 0.20 mM.

Table 2. Effect of benzenedicarboxylic acid (BA) on the length, width, and aspect ratio of $\alpha\text{-CaSO}_4 \cdot 0.5\text{H}_2\text{O}$ particles.

BA Concentration/(mM)	Average Length/ μm	Average Width/ μm	Aspect Ratio	
PA	0	59.04 ± 14.08	11.04 ± 3.64	5.74 ± 1.84
	0.07	42.56 ± 10.02	16.09 ± 3.55	2.72 ± 0.70
	0.13	39.39 ± 9.63	18.02 ± 4.91	2.36 ± 0.91
	0.20	32.19 ± 6.87	20.73 ± 5.26	1.61 ± 0.39
IPA	0.20	41.83 ± 12.72	10.60 ± 3.81	4.24 ± 1.43
TA	0.20	40.30 ± 11.51	9.46 ± 2.96	4.54 ± 1.60

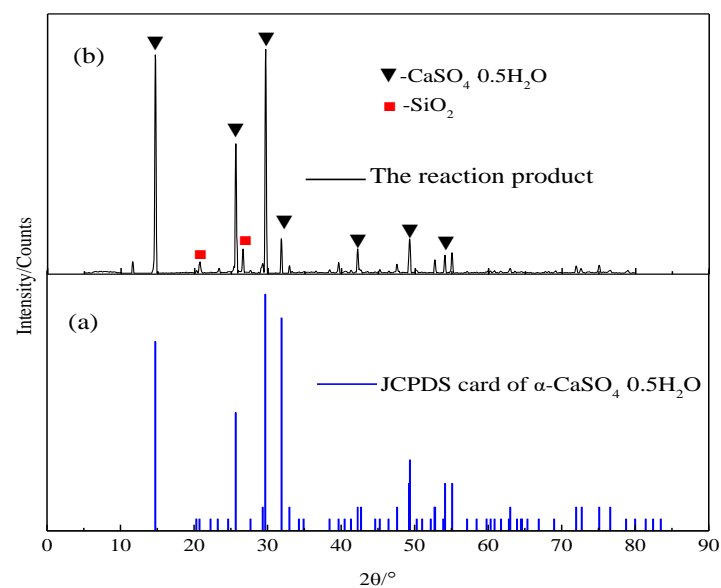


Figure 3. XRD patterns of (a) the JCPDS card of $\alpha\text{-CaSO}_4 \cdot 0.5\text{H}_2\text{O}$ and (b) the reaction product prepared without organic acid.

The effect of the BA concentration on the compressive strength of hardened gypsum ($\text{CaSO}_4 \cdot 2\text{H}_2\text{O}$) hydrated from $\alpha\text{-CaSO}_4 \cdot 0.5\text{H}_2\text{O}$ is shown in Figure 4. As shown in Figure 4, it is beneficial to improve the compressive strength of $\alpha\text{-CaSO}_4 \cdot 0.5\text{H}_2\text{O}$ prepared with PA. Compared with the blank experiment, the compressive strength increased from 13.1 MPa to 22.5 MPa with a PA concentration of 0.20 mM. However, when the concentration of IPA or TA was 0.20 mM, the compressive strength was only 10 MPa. Therefore, the addition of IPA or TA cannot improve the mechanical strength of $\alpha\text{-CaSO}_4 \cdot 0.5\text{H}_2\text{O}$, and they are not appropriate as crystal modifiers for the preparation of $\alpha\text{-CaSO}_4 \cdot 0.5\text{H}_2\text{O}$ by atmospheric salt solution.

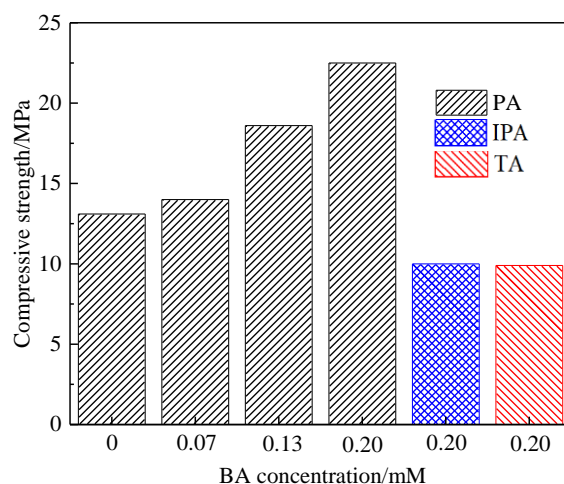


Figure 4. Effect of BA concentration on the compressive strength of $\text{CaSO}_4 \cdot 0.5\text{H}_2\text{O}$.

3.2. Effect of Amino Acid on the Crystal Habit of $\alpha\text{-CaSO}_4 \cdot 0.5\text{H}_2\text{O}$

In order to investigate the feasibility of amino acids as crystal modifiers, L-aspartic acid (L-Asp, $\text{HOOC-CH}(\text{NH}_2)\text{-CH}_2\text{-COOH}$), L-glutamic acid (L-Glu, $\text{HOOC-CH}(\text{NH}_2)\text{-(CH}_2)_2\text{-COOH}$), and L-asparagine (L-Asn, $\text{O=C}(\text{NH}_2)\text{CH}_2\text{CH}(\text{NH}_2)\text{-COOH}$) were applied to regulate the crystal habit of $\alpha\text{-CaSO}_4 \cdot 0.5\text{H}_2\text{O}$. The molecular structural formulas are shown in Figure 5. The L-Asp contains one NH_2 and two COOH , and the two COOH are separated by a $\text{-CH}_2\text{-CH}(\text{NH}_2)\text{-}$ group. Compared with the L-Asp, the only difference is that the two COOH are separated by a $\text{-(CH}_2)_2\text{-CH}(\text{NH}_2)\text{-}$ group for the L-Glu molecule. The L-Asn contains a COOH and a C=O , and the two functional groups are separated by a $\text{-CH}_2\text{-CH}(\text{NH}_2)\text{-}$ group. In fact, the only difference between L-Asn and L-Asp is a NH_2 instead of an OH linked to the C=O function. Although we reported earlier that L-Asp is an effective crystal modifier [24], L-Glu and L-Asn with similar structures have not been investigated.

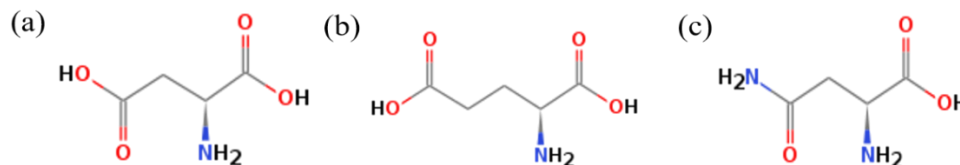


Figure 5. Molecular structural formulas of (a) L-Asp, (b) L-Glu, and (c) L-Asn.

The crystal habit and size variations of $\alpha\text{-CaSO}_4 \cdot 0.5\text{H}_2\text{O}$ at different amino acid concentrations are presented in Figures 6 and 7, respectively. Clearly, the crystal habit of $\alpha\text{-CaSO}_4 \cdot 0.5\text{H}_2\text{O}$ is significantly affected by L-Asp. In the presence of 2.50 mM L-Asp, the average width of $\alpha\text{-CaSO}_4 \cdot 0.5\text{H}_2\text{O}$ particles increased to $27.63 \pm 7.52 \mu\text{m}$, and the aspect ratio decreased to 1.21 ± 0.30 . Therefore, it is inferred that L-Asp has the ability to control the crystal habit of $\alpha\text{-CaSO}_4 \cdot 0.5\text{H}_2\text{O}$. Interestingly, although the concentrations of L-Glu and L-Asn were obviously greater than that of L-Asp, they could not change the crystal habit of $\alpha\text{-CaSO}_4 \cdot 0.5\text{H}_2\text{O}$. The average width was about $11 \mu\text{m}$, and the range of aspect

ratio was 5–6. Like IPA, even if the L-Glu contains two COOH, it cannot regulate the crystal habit of α -CaSO₄·0.5H₂O from acicular crystal to short columnar crystal when the two COOH are separated by more than two methylene/methine groups. Inversely, Teng et al. [27] synthesized α -CaSO₄·0.5H₂O whiskers with high aspect ratios of 200 at atmospheric pressure with the assistance of L-Glu. Therefore, the L-Glu is unable to convert the morphology of α -CaSO₄·0.5H₂O from needle-like shape to a short columnar shape. Furthermore, although the COOH and C=O are separated by a –CH₂–CH(NH₂)– group like the L-Asp, L-Asn also cannot regulate the crystal habit of α -CaSO₄·0.5H₂O because the NH₂ group does not have the same role as the OH group. Similarly, Tan et al. [22] found that long columnar crystals with uniform diameters could be obtained by adding acrylic acid (CH₂=CH–COOH), which contained only one COOH and could not convert the α -CaSO₄·0.5H₂O from long columnar whiskers to short columnar crystals. However, the crystal habit of α -CaSO₄·0.5H₂O can be controlled by citric acid and ethylene diamine tetraacetic acid (EDTA) [28], which contain three and four COOH, respectively. Thus, it can be concluded that the crystal modifier must contain two or more COOH, and the separation between two COOH in the crystal modifier molecule cannot be more than two methylene/methine groups.

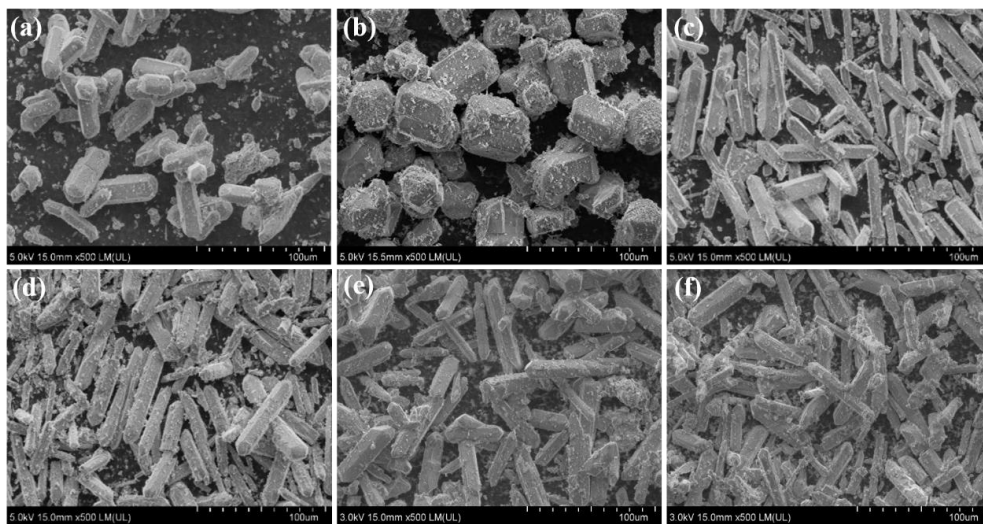


Figure 6. Effect of amino acid concentration on the crystal habit of CaSO₄·0.5H₂O. (a) L-Asp: 1.25 mM; (b) L-Asp: 2.50 mM; (c) L-Glu: 4.44 mM; (d) L-Glu: 8.88 mM; (e) L-Asn: 2.52 mM; (f) L-Asn: 12.60 mM.

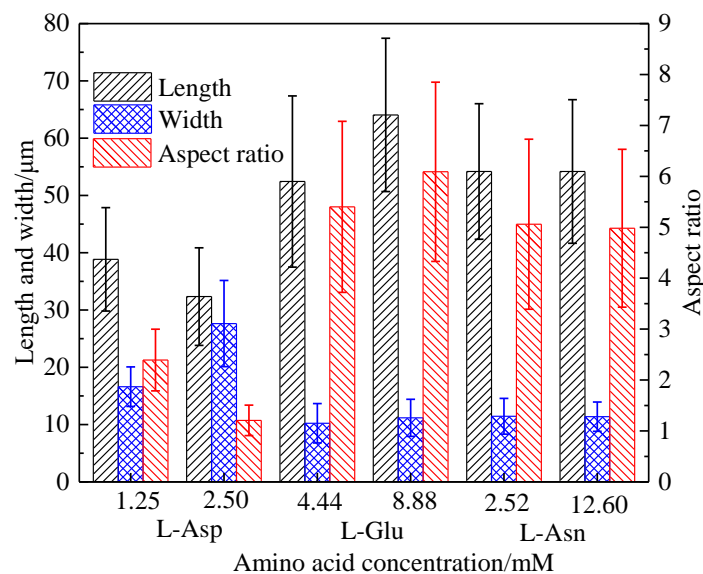


Figure 7. Effect of amino acids on the length, diameter, and aspect ratio of CaSO₄·0.5H₂O.

The effect of L-Asp, L-Glu, and L-Asn on the compressive strength of the hardened pastes hydrated from $\alpha\text{-CaSO}_4\cdot 0.5\text{H}_2\text{O}$ is shown in Figure 8. The results show that the compressive strength increases with an increase in the L-Asp concentration. In the presence of 2.50 mM L-Asp, the compressive strength of $\alpha\text{-CaSO}_4\cdot 0.5\text{H}_2\text{O}$ reached 30.2 MPa. On the contrary, the compressive strength decreased along with the increase in L-Glu or L-Asn concentrations, with the value being lower than 10 MPa. Therefore, the addition of L-Glu or L-Asn does not improve the mechanical strength.

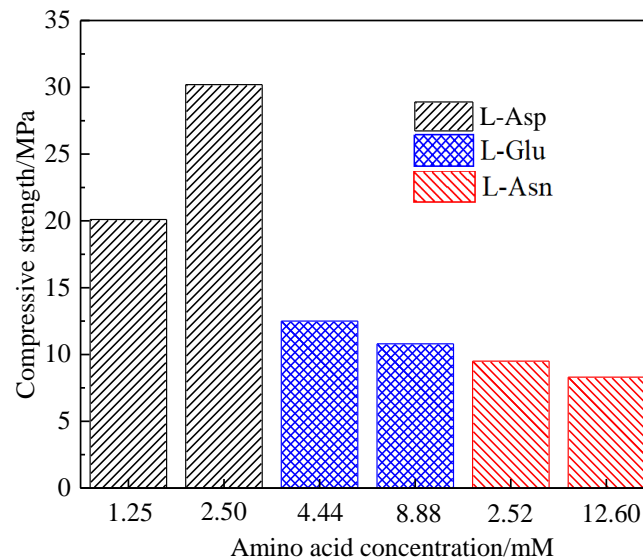


Figure 8. Effect of amino acid concentration on the compressive strength of $\text{CaSO}_4\cdot 0.5\text{H}_2\text{O}$.

3.3. Effect of Straight-Chain Dicarboxylic Acid on the Crystal Habit of $\alpha\text{-CaSO}_4\cdot 0.5\text{H}_2\text{O}$

Dicarboxylic acids with different lengths of carbon chain such as oxalic acid (OA), propanedioic acid (PD), succinic acid (SA), and maleic acid (MA) are shown in Figure 9. What these dicarboxylic acids all have in common is that they contain two COOH, but the separation between the two COOH are different, being separated by zero, one methylene group, and two methylene groups for OA, PD, and SA, respectively. Compared with SA, the only difference in the MA is that it contains a double bond.

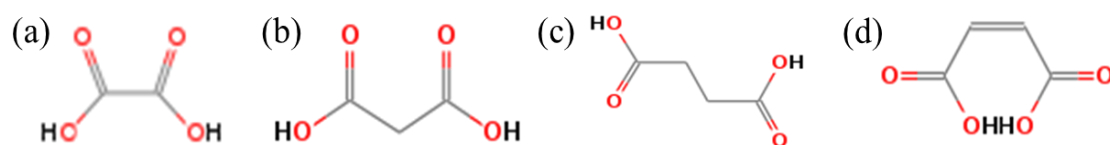


Figure 9. Molecular structural formula of (a) OA, (b) PD, (c) SA and (d) MA.

The effect of dicarboxylic acids on the crystal habit of $\alpha\text{-CaSO}_4\cdot 0.5\text{H}_2\text{O}$ is presented in Figure 10, and the corresponding length, width, and aspect ratio are shown in Table 3. In the presence of 0.11 mM OA and PD, the corresponding aspect ratios of $\alpha\text{-CaSO}_4\cdot 0.5\text{H}_2\text{O}$ particles were 5.58 ± 1.85 and 5.19 ± 1.45 , respectively, with the average width of 10 μm . Therefore, the OA and PD cannot regulate the crystal habit of $\alpha\text{-CaSO}_4\cdot 0.5\text{H}_2\text{O}$, and we can infer that the separation between the two COOH in the crystal modifier molecule cannot be lower than two methylene groups. The results agree with previously studies, for example, Liu et al. [29] also found that OA did not modify the crystal morphology of $\alpha\text{-CaSO}_4\cdot 0.5\text{H}_2\text{O}$, which was still acerosc or linear clavate, and the crystal morphology of $\alpha\text{-CaSO}_4\cdot 0.5\text{H}_2\text{O}$ had no significant changes with the addition of PD. However, when the concentration of SA was 0.11 mM, the average width enlarged to $17.67 \pm 6.71 \mu\text{m}$, and the aspect ratio decreases to 3.12 ± 1.10 . With a further increase in SA concentration to 0.22 mM, the particle size of $\alpha\text{-CaSO}_4\cdot 0.5\text{H}_2\text{O}$ decreased rapidly, the average width reduced to $1.47 \pm 0.54 \mu\text{m}$, and the aspect ratio reached up to 9.40 ± 3.10 . When the concentration of MA was 0.17 mM, the average width

enlarged to $18.15 \pm 7.24 \mu\text{m}$, with the lower aspect ratio of 2.42 ± 1.09 . Hence, SA and MA can be used as crystal modifiers, and the cis-conformation MA shows a better control effect. The reason is that the double bond helps to improve the complexing electron coordination ability of COOH and Ca on the crystal surface of $\alpha\text{-CaSO}_4 \cdot 0.5\text{H}_2\text{O}$ [30,31]. Furthermore, the concentration of SA should be controlled within a certain range.

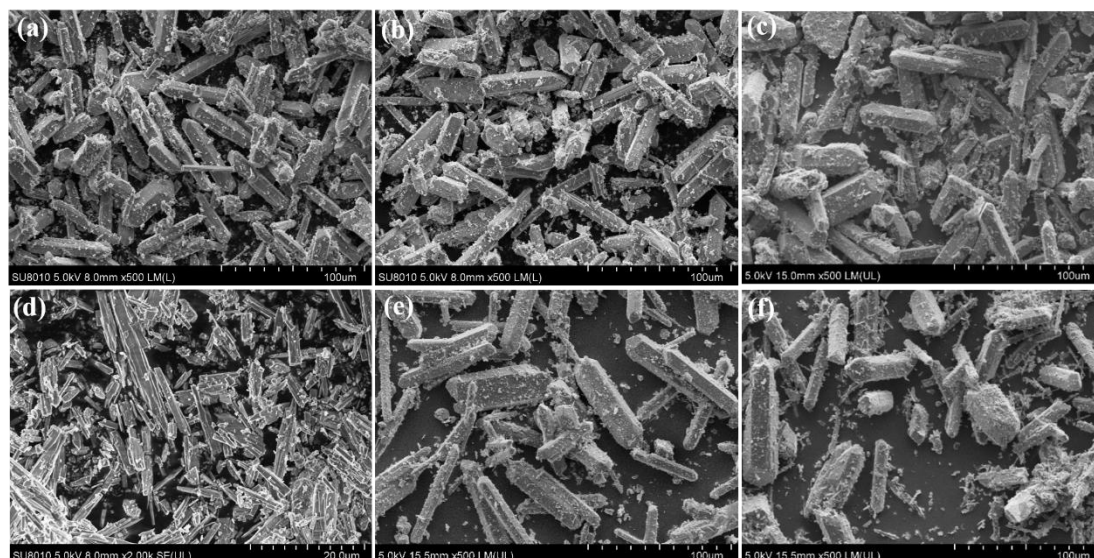


Figure 10. Effect of straight-chain dicarboxylic acid on the crystal habit of $\text{CaSO}_4 \cdot 0.5\text{H}_2\text{O}$. (a) OA: 0.11 mM; (b) PD: 0.11 mM; (c) SA: 0.11 mM; (d) SA: 0.22 mM; (e) MA: 0.06 mM; (f) MA: 0.17 mM.

Table 3. Effect of straight-chain dicarboxylic acid on the length, diameter, and aspect ratio of $\alpha\text{-CaSO}_4 \cdot 0.5\text{H}_2\text{O}$ particles.

Dicarboxylic Acids	Concentration/mM	Average Length/ μm	Average Width/ μm	Aspect Ratio
OA	0.11	51.31 ± 12.17	9.86 ± 2.74	5.58 ± 1.85
PD	0.11	51.87 ± 10.17	10.53 ± 2.75	5.19 ± 1.45
SA	0.11	50.14 ± 10.87	17.67 ± 6.71	3.12 ± 1.10
	0.22	13.89 ± 7.33	1.47 ± 0.54	9.40 ± 3.10
MA	0.06	59.19 ± 11.11	13.68 ± 4.10	4.68 ± 1.52
	0.17	39.35 ± 14.69	18.15 ± 7.24	2.42 ± 1.09

The effect of OA, PD, SA, and MA on the compressive strength of hardened pastes is shown in Figure 11. The results show that the compressive strength of $\alpha\text{-CaSO}_4 \cdot 0.5\text{H}_2\text{O}$ prepared with OA and PD was less than 10 MPa. Hence, the addition of OA or PD does not improve the mechanical strength. It is worth noting that the compressive strength increased to 25.3 MPa in the presence of 0.11 mM SA, but with a further increase in SA concentration to 0.22 mM, the particle size and compressive strength of $\alpha\text{-CaSO}_4 \cdot 0.5\text{H}_2\text{O}$ sharply decreased. In addition, the compressive strength of $\alpha\text{-CaSO}_4 \cdot 0.5\text{H}_2\text{O}$ prepared with 0.17 mM MA reached 30.4 MPa.

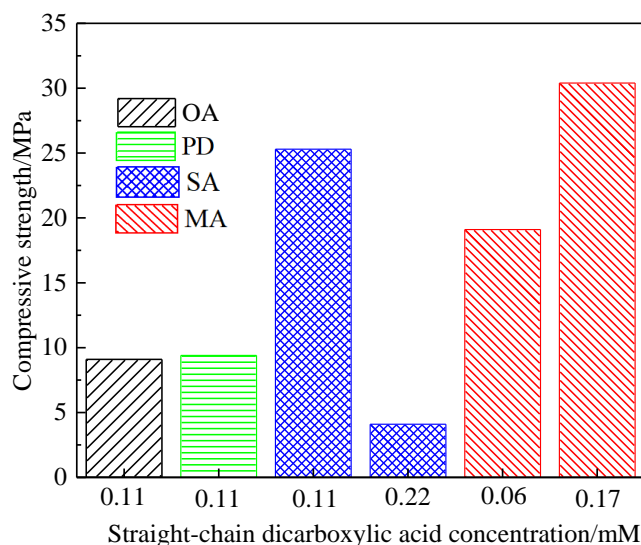


Figure 11. Effect of straight-chain dicarboxylic acid concentration on the compressive strength of α -CaSO₄·0.5H₂O.

In conclusion, when the separation between the two COOH in the molecular structure of organic acids is lower or higher than two methylene or methine groups and the number of COOH is less than two, the organic acids do not have the ability to regulate the crystal habit of α -CaSO₄·0.5H₂O. That is to say, the molecular structure characteristics of organic acid crystal modifiers are that they contain two or more COOH and the two COOH are separated by two methylene or methine groups.

3.4. Control Mechanism of Organic Acids for the Crystal Habit of α -CaSO₄·0.5H₂O

The FTIR spectra of α -CaSO₄·0.5H₂O particles prepared with different crystal modifiers are presented in Figure 12. As shown in Figure 12a, the peak at 1622 cm⁻¹ belongs to the bending vibrations of water molecules in α -CaSO₄·0.5H₂O, and the two peaks positioned at 3557 cm⁻¹ and 3610 cm⁻¹ are attributed to the O–H stretching vibration [32]. The peak at 466 cm⁻¹ is the symmetrical bending vibration of ν_2 SO₄²⁻. The peaks located at 1152 cm⁻¹ and 1093 cm⁻¹ are ascribed to the asymmetrical stretching vibration of ν_3 SO₄²⁻. The peaks at 660 cm⁻¹ and 599 cm⁻¹ are the asymmetrical bending vibrations of ν_4 SO₄²⁻ [33]. In addition, the peak at 799 cm⁻¹ is the stretching vibration peak of P–O [22].

The spectra of α -CaSO₄·0.5H₂O prepared with L-Asp are presented in Figure 12b. The peak appearing at 1443 cm⁻¹ can be assigned to the symmetric stretching vibration of COO⁻ in amino acid. The peak located at 779 cm⁻¹ is due to the bending vibration of COO⁻, which is considered to be the characteristic absorption peak of short-chain fatty acids [24]. As can be seen from Figure 12c,d, the peak at 1421 cm⁻¹ is the symmetric stretching vibration peak of COO⁻, indicating that the crystal modifiers have been adsorbed on the surface of the α -CaSO₄·0.5H₂O particles.

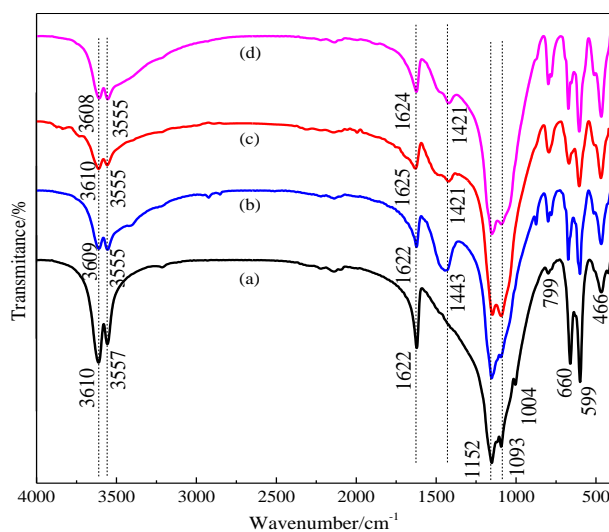


Figure 12. Fourier transform infrared spectroscopy (FTIR) spectra of $\text{CaSO}_4 \cdot 0.5\text{H}_2\text{O}$ particles prepared with different crystal modifiers. (a) Blank test; (b) L-Asp; (c) PA; and (d) MA.

As PD, IPA, L-Glu, and L-Asn do not have the ability to control the crystal shape of $\alpha\text{-CaSO}_4 \cdot 0.5\text{H}_2\text{O}$ particles, FTIR was also used to analyze the adsorption of these organic acids on the surface of $\alpha\text{-CaSO}_4 \cdot 0.5\text{H}_2\text{O}$. The results are shown in Figure 13. Compared with the FTIR spectra of $\alpha\text{-CaSO}_4 \cdot 0.5\text{H}_2\text{O}$ prepared without a crystal modifier, the positions and numbers of the characteristic absorption peaks of $\alpha\text{-CaSO}_4 \cdot 0.5\text{H}_2\text{O}$ prepared with PD, IPA, L-Glu, and L-Asn did not change, indicating that they could not be adsorbed onto the surface of $\alpha\text{-CaSO}_4 \cdot 0.5\text{H}_2\text{O}$ particles or adsorbed by physical absorption.

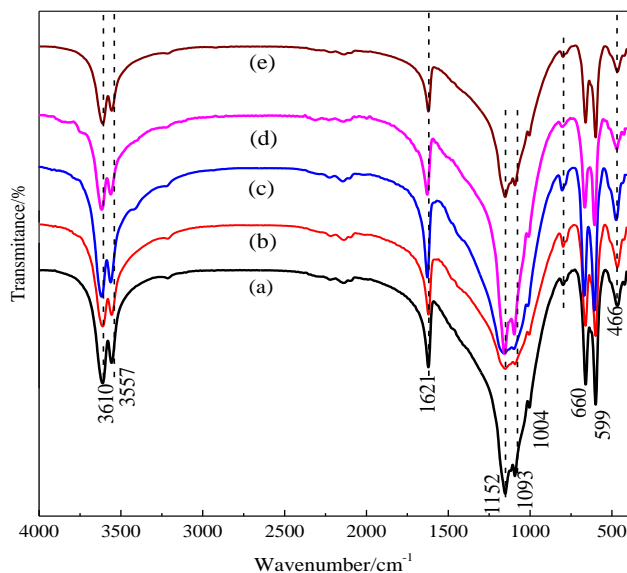


Figure 13. FTIR spectra of $\text{CaSO}_4 \cdot 0.5\text{H}_2\text{O}$ particles prepared with different organic acids. (a) Blank test; (b) PD; (c) IPA; (d) L-Glu; and (e) L-Asn.

To further reveal the microcosmic differences between organic acids with and without the ability to regulate the crystal habit of $\alpha\text{-CaSO}_4 \cdot 0.5\text{H}_2\text{O}$, the separation between the COOH ($d_{\text{COOH-COOH}}$) in different organic acids was measured using the Cambridge Serial Total Energy Package (CASTEP) of Materials Studio 8.0 software based on the density functional theory (DFT), the results of which are shown in Table 4. As can be seen from Table 4, the $d_{\text{COOH-COOH}}$ of crystal modifiers with the ability to regulate the shape of $\alpha\text{-CaSO}_4 \cdot 0.5\text{H}_2\text{O}$ such as SA, MA, PA, and L-Asp were 4.327 Å, 3.785 Å,

3.946 Å, and 4.154 Å, respectively, which were close to the separation between Ca atoms ($d_{\text{Ca-Ca}} = 4.187$ Å) on the end surface of $\alpha\text{-CaSO}_4 \cdot 0.5\text{H}_2\text{O}$ (1 1 1), and the difference value ($\Delta d = d_{\text{Ca-Ca}} - d_{\text{COOH-COOH}}$) was not more than 0.5 Å. However, the $d_{\text{COOH-COOH}}$ of OA and PD were obviously less than 4.187 Å, and the Δd values reached 1.517 Å and 1.322 Å, respectively. Conversely, the $d_{\text{COOH-COOH}}$ of IPA, TA, and L-Glu were significantly greater than $d_{\text{Ca-Ca}}$, and the Δd values reached 0.933 Å, 2.831 Å, and 1.746 Å, respectively. Therefore, when the $d_{\text{COOH-COOH}}$ of organic acids is distinctly lower (Figure 14a) or higher than (Figure 14b) $d_{\text{Ca-Ca}}$, the organic acids cannot interact with Ca atoms on the (111) face of $\alpha\text{-CaSO}_4 \cdot 0.5\text{H}_2\text{O}$, and only when the $d_{\text{COOH-COOH}}$ matches the $d_{\text{Ca-Ca}}$ do the organic acids possess the ability to regulate the crystal habit of $\alpha\text{-CaSO}_4 \cdot 0.5\text{H}_2\text{O}$. Similarly, Badens et al. [26] found that the separation between calcium ions of the faces (120) and (111) of crystal gypsum (4.0 Å) matched the distance between two oxygen ions of the two carboxylic groups of the molecule of citric acid and MA, and the distance between the two oxygen ions of the active sites was much more important than the distance of two first neighbors of calcium ions on the gypsum crystal. Furthermore, although the $d_{\text{COOH-C=O}}$ of L-Asn (4.073 Å) was close to $d_{\text{Ca-Ca}}$, the L-Asn contained only one COOH, so it cannot stably adsorb on the (111) face by two COOH. These analysis results are in agreement with the SEM observation and FTIR tests.

Table 4. COOH separation of different organic acids.

Organic Acid	OA	PD	SA	MA	PA	IPA	TA	L-Asp	L-Asn	L-Glu
COOH separation /Å	2.670	2.865	4.327	3.785	3.946	5.120	7.018	4.154	4.073	5.933

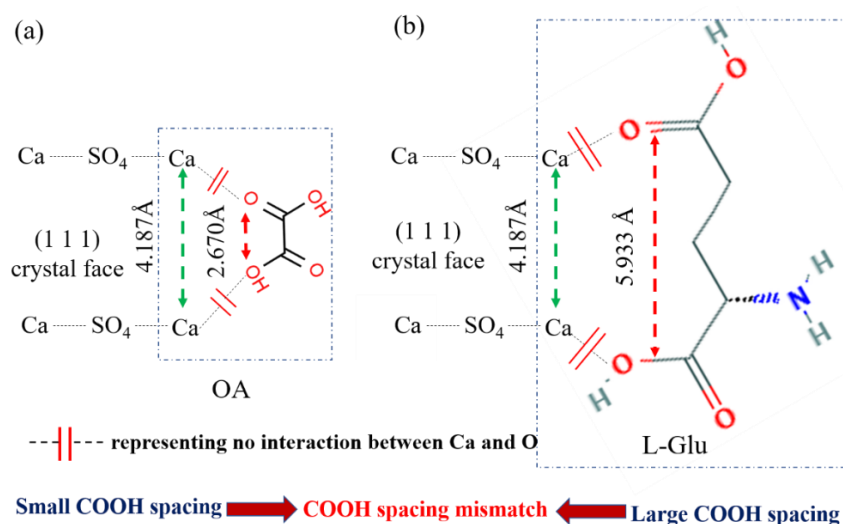


Figure 14. Schematic diagram of OA (a) and L-Glu (b) on the (111) surface of $\text{CaSO}_4 \cdot 0.5\text{H}_2\text{O}$.

The model of $\alpha\text{-CaSO}_4 \cdot 0.5\text{H}_2\text{O}$ crystal habit regulated by the crystal modifier is shown in Figure 15. In our previous study, the adsorption of the MA molecule on the (111), (110), and (010) crystal faces of $\alpha\text{-CaSO}_4 \cdot 0.5\text{H}_2\text{O}$ were studied using DFT calculations, and the results indicated that the (111) face was the most stable chemical adsorption surface and presented the strongest bonding interaction with MA, and the adsorption of MA on the (110) and (010) faces was relatively weak [21]. Therefore, the crystal modifier can preferentially adsorb on the (111) face and retard its growth in the length direction. Moreover, with an increase in the crystal modifier concentration, the $\alpha\text{-CaSO}_4 \cdot 0.5\text{H}_2\text{O}$ crystals are shortened in length and enlarged in width, resulting in the decrease in aspect ratio.

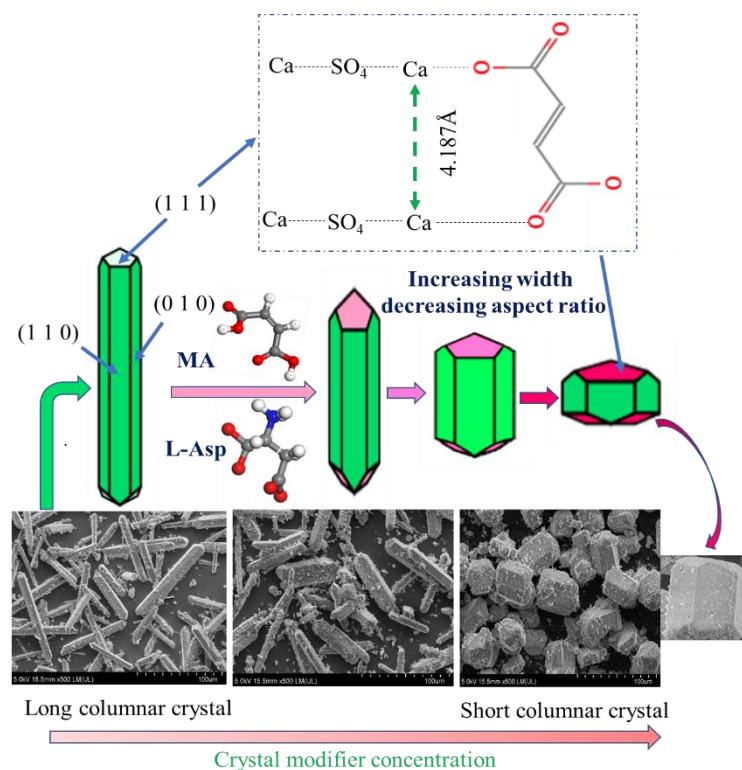


Figure 15. Model of $\text{CaSO}_4 \cdot 0.5\text{H}_2\text{O}$ crystal habit regulated by the crystal modifier.

4. Conclusions

Organic acids with different molecular structures were adopted to regulate the crystal habit of $\alpha\text{-CaSO}_4 \cdot 0.5\text{H}_2\text{O}$, and the adsorption differences of organic acids on the surface of $\alpha\text{-CaSO}_4 \cdot 0.5\text{H}_2\text{O}$ particles were clarified. The conclusions are as follows.

The molecular structure characteristics of organic acid crystal modifiers are that they contain two or more COOH and that the two COOH are separated by two methylene or methine groups. The crystal modifiers can adsorb on the surface of $\alpha\text{-CaSO}_4 \cdot 0.5\text{H}_2\text{O}$ particles and change its growth habit. With the increase in the crystal modifier concentration such as PA, L-Asp, SA, and MA, the $\alpha\text{-CaSO}_4 \cdot 0.5\text{H}_2\text{O}$ crystals are shortened in length and enlarged in width, resulting in the decrease in aspect ratio and the increase in compressive strength. Organic acids without the control ability such as PD, IPA, L-Glu, and L-Asn neither adsorb on the surface of $\alpha\text{-CaSO}_4 \cdot 0.5\text{H}_2\text{O}$ particles, nor change its crystal habit and improve the compression strength.

Author Contributions: X.L. performed the experiments and wrote the manuscript. Q.Z. conceived and designed the experiments. All authors have read and agreed to the published version of the manuscript.

Funding: This research was funded by the National Natural Science Foundation of China, grant number U1812402.

Conflicts of Interest: The authors declare no conflicts of interest.

References

1. Hammas, I.; Horchani-Naifer, K.; Férid, M. Solubility study and valorization of phosphogypsum salt solution. *Int. J. Miner. Process.* **2013**, *123*, 87–93. [[CrossRef](#)]
2. Romero-Hermida, I.; Morales-Flórez, V.; Santos, A.; Villena, A.; Esquivias, L. Technological proposals for recycling industrial wastes for environmental applications. *Minerals-Basel* **2014**, *4*, 746–757. [[CrossRef](#)]
3. Rashad, A.M. Phosphogypsum as a construction material. *J. Clean. Prod.* **2017**, *166*, 732–743. [[CrossRef](#)]
4. Islam, G.M.S.; Chowdhury, F.H.; Raihan, M.T.; Amit, S.K.S.; Islam, M.R. Effect of phosphogypsum on the properties of portland cement. *Procedia Eng.* **2017**, *171*, 744–751. [[CrossRef](#)]

5. Hua, S.D.; Wang, K.J.; Yao, X. Developing high performance phosphogypsum-based cementitious materials for oil-well cementing through a step-by-step optimization method. *Cem. Concr. Compos.* **2016**, *72*, 299–308. [[CrossRef](#)]
6. Yang, L.; Zhang, Y.S.; Yan, Y. Utilization of original phosphogypsum as raw material for the preparation of self-leveling mortar. *J. Clean. Prod.* **2016**, *127*, 204–213. [[CrossRef](#)]
7. Ye, X.D. Current situation, existing problems and suggestions of phosphogypsum utilization in China in 2018. *Phosphate Compound Fert.* **2018**, *34*, 1–4.
8. Jiang, G.M.; Wang, H.; Chen, Q.S.; Zhang, X.M.; Wu, Z.B.; Guan, B.H. Preparation of alpha-calcium sulfate hemihydrate from FGD gypsum in chloride-free $\text{Ca}(\text{NO}_3)_2$ solution under mild conditions. *Fuel* **2016**, *174*, 235–241. [[CrossRef](#)]
9. Guan, B.H.; Yang, L.; Fu, H.L.; Kong, B.; Li, T.Y.; Yang, L.C. α -calcium sulfate hemihydrate preparation from FGD gypsum in recycling mixed salt solutions. *Chem. Eng. J.* **2011**, *174*, 296–303. [[CrossRef](#)]
10. Zhang, R.; Li, Y.J.; Liu, J.; Zhao, Y.Y.; Jiang, Y.D. Utilization of phosphogypsum and treatment of the impure elements. *Conserv. Utilization Miner. Resour.* **2015**, 50–54. [[CrossRef](#)]
11. Guan, Q.J.; Sun, W.; Hu, Y.H.; Yin, Z.G.; Zhang, C.H.; Guan, C.P.; Zhu, X.N.; Ahmed Khoso, S. Simultaneous control of particle size and morphology of α - $\text{CaSO}_4 \cdot \frac{1}{2}\text{H}_2\text{O}$ with organic additives. *J. Am. Ceram. Soc.* **2019**, *102*, 2441–2449.
12. Shen, Z.X.; Guan, B.H.; Fu, H.L.; Yang, L.C. Effect of potassium sodium tartrate and sodium citrate on the preparation of α -calcium sulfate hemihydrate from flue gas desulfurization gypsum in a concentrated electrolyte solution. *J. Am. Ceram. Soc.* **2009**, *92*, 2894–2899. [[CrossRef](#)]
13. Duan, Z.Y.; Li, J.X.; Li, T.G.; Zheng, S.R.; Han, W.M.; Geng, Q.Y.; Guo, H.B. Influence of crystal modifier on the preparation of α -hemihydrate gypsum from phosphogypsum. *Constr. Build. Mater.* **2017**, *133*, 323–329. [[CrossRef](#)]
14. Li, F.; Liu, J.L.; Yang, G.Y.; Pan, Z.Y.; Ni, X.; Xu, H.; Huang, Q. Effect of pH and succinic acid on the morphology of α -calcium sulfate hemihydrate synthesized by a salt solution method. *J. Cryst. Growth* **2013**, *374*, 31–36. [[CrossRef](#)]
15. Guan, Q.J.; Sun, W.; Hu, Y.H.; Yin, Z.G.; Guan, C.P. Synthesis of α - $\text{CaSO}_4 \cdot 0.5\text{H}_2\text{O}$ from flue gas desulfurization gypsum regulated by $\text{C}_4\text{H}_4\text{O}_4\text{Na}_2 \cdot 6\text{H}_2\text{O}$ and NaCl in glycerol-water solution. *RSC Adv.* **2017**, *7*, 27807–27815. [[CrossRef](#)]
16. Guan, Q.J.; Tang, H.H.; Sun, W.; Hu, Y.H.; Yin, Z.G. Insight into influence of glycerol on preparing α - $\text{CaSO}_4 \cdot 1/2\text{H}_2\text{O}$ from flue gas desulfurization gypsum in glycerol-water solutions with succinic acid and NaCl. *Ind. Eng. Chem. Res.* **2017**, *56*, 9831–9838. [[CrossRef](#)]
17. Mi, Y.; Chen, D.Y.; Wang, S.Z. Utilization of phosphogypsum for the preparation of α -calcium sulfate hemihydrate in chloride-free solution under atmospheric pressure. *J. Chem. Technol. Biotechnol.* **2018**, *93*, 2371–2379. [[CrossRef](#)]
18. Shao, D.D.; Zhao, B.; Zhang, H.Q.; Wang, Z.G.; Shi, C.J.; Cao, J.L. Preparation of large-grained α -high strength gypsum with FGD gypsum. *Cryst. Res. Technol.* **2017**, *52*, 1700078. [[CrossRef](#)]
19. Lu, W.D.; Ma, B.G.; Su, Y.; He, X.Y.; Jin, Z.; Qi, H.H. Preparation of α -hemihydrate gypsum from phosphogypsum in recycling CaCl_2 solution. *Constr. Build. Mater.* **2019**, *214*, 399–412. [[CrossRef](#)]
20. Guan, B.H.; Kong, B.; Fu, H.L.; Yu, J.; Jiang, G.M.; Yang, L. Pilot scale preparation of α -calcium sulfate hemihydrate from FGD gypsum in Ca–K–Mg aqueous solution under atmospheric pressure. *Fuel* **2012**, *98*, 48–54. [[CrossRef](#)]
21. Li, X.B.; Zhang, Q.; Ke, B.L.; Wang, X.C.; Li, L.J.; Li, X.H.; Mao, S. Insight into the effect of maleic acid on the preparation of α -hemihydrate gypsum from phosphogypsum in Na_2SO_4 solution. *J. Cryst. Growth* **2018**, *493*, 34–40. [[CrossRef](#)]
22. Tan, H.; Dong, F. Morphological regulation of calcium sulfate hemihydrate from phosphogypsum. *Materialwissenschaft und Werkstofftechnik* **2017**, *48*, 1191–1196. [[CrossRef](#)]
23. Ma, B.G.; Lu, W.D.; Su, Y.; Li, Y.B.; Gao, C.; He, X.Y. Synthesis of α -hemihydrate gypsum from cleaner phosphogypsum. *J. Clean. Prod.* **2018**, *195*, 396–405. [[CrossRef](#)]
24. Li, X.B.; Zhang, Q.; Shen, Z.H.; Li, L.J.; Li, X.H.; Mao, S. L-aspartic acid: A crystal modifier for preparation of hemihydrate from phosphogypsum in CaCl_2 solution. *J. Cryst. Growth* **2019**, *511*, 48–55. [[CrossRef](#)]
25. Wang, X.S.; Zhou, M.; Ke, X.; Tan, R.Q.; Chen, Y.C.; Hou, H.B. Synthesis of alpha hemihydrate particles with lithium and carboxylates via the hydrothermal method. *Powder Technol.* **2017**, *317*, 293–300. [[CrossRef](#)]

26. Badens, E.; Veessler, S.; Boistelle, R. Crystallization of gypsum from hemihydrate in presence of additives. *J. Cryst. Growth* **1999**, *198*, 704–709. [[CrossRef](#)]
27. Teng, W.; Wang, J.; Wu, J.; Du, Y.; Jia, X.; Li, H.; Wang, T. Rapid synthesis of alpha calcium sulfate hemihydrate whiskers in glycerol-water solution by using flue-gas-desulfurization gypsum solid waste. *J. Cryst. Growth* **2018**, *496–497*, 24–30. [[CrossRef](#)]
28. Jia, C.Y.; Chen, Q.S.; Zhou, X.; Wang, H.; Jiang, G.M.; Guan, B.H. Trace NaCl and Na₂EDTA mediated synthesis of α -calcium sulfate hemihydrate in glycerol–water solution. *Ind. Eng. Chem. Res.* **2016**, *55*, 9189–9194. [[CrossRef](#)]
29. Liu, X.F.; Peng, J.H.; Zhang, J.X.; Qu, J.D.; Li, M. Effect of organic diacid carbon chain length on crystal morphology of α -calcium sulfate hemihydrate in preparation from flue gas desulphurization gypsum. *Appl. Mech. Mater.* **2012**, *253–255*, 542–545. [[CrossRef](#)]
30. Zhao, Z.M.; Luan, Y.; Quan, S.C.; Wu, J.L. The effect of functional groups for the organic acid on the crystal transition of phosphogypsum crystal. *J. Build. Mater.* **2018**, *21*, 247–252.
31. Peng, J.H.; Chen, M.F.; Zhang, J.X.; Qu, J.D.; Zou, C.Y. Influence of organic acid structure on crystal morphology of α -hemihydrate desulfurization gypsum and Its crystal modification mechanism. *J. Sichuan Univ. (Eng. Sci. Ed.)* **2012**, *44*, 116–172.
32. Mandal, P.K.; Mandal, T.K. Anion water in gypsum (CaSO₄·2H₂O) and hemihydrate (CaSO₄·1/2H₂O). *Cem. Concr. Res.* **2002**, *32*, 313–316. [[CrossRef](#)]
33. Mao, J.W.; Jiang, G.M.; Chen, Q.S.; Guan, B.H. Influences of citric acid on the metastability of α -calcium sulfate hemihydrate in CaCl₂ solution. *Colloid. Surface. A Physicochem. Eng. Asp.* **2014**, *443*, 265–271. [[CrossRef](#)]



© 2020 by the authors. Licensee MDPI, Basel, Switzerland. This article is an open access article distributed under the terms and conditions of the Creative Commons Attribution (CC BY) license (<http://creativecommons.org/licenses/by/4.0/>).